Available online at www.sciencedirect.com

SciVerse ScienceDirect

Ceramics International 39 (2013) 3931–3938

CERAMICS INTERNATIONAL

www.elsevier.com/locate/ceramint

In-situ fabrication of Al_2O_3–SiC nanocomposites using B_2O_3 as sintering aid

S. Rasouli[a], E. Taheri-Nassaj[a,*], S.A. Hassanzadeh-Tabrizi[b]

[a]*Department of Materials Science and Engineering, Tarbiat Modares University, PO Box 14115-143, Tehran, Iran*
[b]*Department of Materials Engineering, Islamic Azad University, Najafabad Branch, Isfahan, Iran*

Received 13 March 2011; received in revised form 16 October 2012; accepted 23 October 2012
Available online 24 November 2012

Abstract

Al_2O_3–SiC nanocomposites with 5 and 10 vol% SiC have been in-situ fabricated by sol-gel method followed by carbothermal reduction of alumina–silica gel using B_2O_3 as sintering aid. Green bodies were formed by cold isostatic pressing of calcined gel, which was prepared by an aqueous sol-containing aluminum chloride, TEOS, sucrose and boric acid. Pressureless sintering was carried out in Ar–12%H_2 atmosphere at 1700 °C. Addition of B_2O_3 (1 or 3 wt%) was an effective densification aid in the Al_2O_3–5 vol% SiC composites, while the densification of Al_2O_3–10 vol% SiC composites was not affected by adding B_2O_3. The composite material containing 5 vol% SiC doped with 3 wt% B_2O_3 reached 98.7% of full density. Nano-sized β-SiC particles were formed in-situ by means of a reaction between mullite and carbon at 1600 °C. Scanning electron microscopy revealed that the spherical in-situ synthesized SiC nanoparticles were well distributed through the composite and located predominantly to the interior of alumina matrix grains.
© 2012 Elsevier Ltd and Techna Group S.r.l. All rights reserved.

Keywords: Nanocomposites; Sol–gel processes; Al_2O_3; SiC

1. Introduction

Alumina-based ceramic matrix composites reinforced with nano-sized ceramic particles have attracted considerable attention, due to their potential for structural applications [1–4]. It has been reported that the incorporation of a dispersion of second phase nanoparticles with lower thermal expansion coefficient than the matrix can improve the mechanical properties of ceramic materials [1,5–8]. Due to its low thermal expansion, high hardness and low reactivity, SiC is considered among the best reinforcements for ceramic composites [9].

Most of the nanocomposites have been made via conventional powder processing routes, which involve mixing of nano-sized starting powders, followed by pressureless sintering. There will be a risk of agglomeration if the starting material is formed by mixing different powders. Sol-gel processing is, from this point of view, an interesting alternative for the fabrication of high quality nanocomposites. It achieves ultra homogenous dispersion of the second phase particles in the matrix [10–13]. In addition, in-situ synthesis of SiC nanoparticles by using sol–gel method, results in better bonding between SiC nanoparticles and Al_2O_3 matrix grains in sintered samples.

Al_2O_3–SiC nanocomposites have previously been fabricated by mixing of alumina and silicon carbide nanopowders followed by pressureless sintering, hot pressing or spark plasma sintering [6,14–16]. Gustafson et al. [17] synthesized a homogenous distribution of SiC nanoparticles during sintering of an Al_2O_3 powder compact containing SiC precursors. Galusek et al. [18] fabricated Al_2O_3–SiC micro/nano composites by warm pressing of poly(allyl) carbosilane coated submicrometer alumina powder with subsequent pressureless sintering.

It is well established that the inclusion of SiC nanoparticles in the matrix can inhibit the grain growth of alumina, but the particles will also obstruct densification [19–21]. Some researches show that doping with small amount of MgO [14,22] and Y_2O_3[23,24], can be a useful method to enhance the sinterability of alumina-silicon carbide nanocomposites. B_2O_3 can promote the carbothermal reduction

*Corresponding author. Tel.: +982182883306; fax: +982188005040.
E-mail address: taheri@modares.ac.ir (E. Taheri-Nassaj).

0272-8842/$ - see front matter © 2012 Elsevier Ltd and Techna Group S.r.l. All rights reserved.
http://dx.doi.org/10.1016/j.ceramint.2012.10.240

reactions [25,26], and leads to the formation of a liquid phase in Al_2O_3–B_2O_3–SiO_2 system at temperatures lower than the sintering temperature of Al_2O_3–SiC composites [27]. So, it can be an interesting alternative sintering aid for in-situ fabrication of Al_2O_3–SiC composites.

In the present work, Al_2O_3–SiC nanocomposites were in-situ fabricated by reaction sintering of alumina–silica calcined gels prepared from an aqueous suspension of aluminum chloride, TEOS and sucrose. Boric acid was also used as sintering aid. Homogenous green bodies were pressureless sintered in Ar–12%H_2 atmosphere.

2. Experimental procedures

The precursor solutions for Al_2O_3–SiC composite were prepared by sol–gel method using $AlCl_3 \cdot 6H_2O$ (Merck), tetraethylorthosilicate (TEOS) (Merck), nitric acid, sucrose (Merck), ethanol and H_3BO_3. First, sucrose was dissolved in deionized water and ethanol, then aluminum chloride hexahydrate was added to the solution. Subsequently the precursor solution was stirred at 60 °C for 30 min. In this stage, TEOS, nitric acid and H_3BO_3 were added and the main solution was continuously stirred at 90 °C for 18 h. The viscosity of the batch gradually increased and finally the batch set to a rigid gel. Then it was dried for 24 h in air at 60 °C, and ball-milled in ethanol media using a high dense alumina jar and high pure alumina balls. The powder then calcined at 800 °C for 1 h. Some of the dried gel was heat treated at temperature range of 1250–1600 °C in Ar–12%H_2 atmosphere in order to investigate the phase formations at different temperatures.

After adding pressing aid (3% PVA 2%) to calcined powder and granulation, the spherical granules were hand-pressed into compacts and these were cold isostatically pressed at 450 MPa. The green bodies were placed in a SiC protection powder bed and pressureless sintered in Ar–12%H_2 atmosphere at 1700 °C for 3 h. The reaction sintering was conducted in a high temperature furnace in which a reaction system was designed to control the atmosphere as depicted in Fig. 1. This system consisted of a cylindrical ceramic chamber completely insulated by low heat loss ceramic fibers. Ar–12%H_2 was injected into the chamber through ceramic pipes with the gas flow rate of 0.1 L/min. A certain gas pressure had to be maintained inside the chamber to prevent oxidization of carbonized sucrose and newly formed SiC. The flow chart of the process and the predicted composition of the sintered specimens are depicted in Fig. 2 and Table 1, respectively.

Powder morphology and microstructure of the sintered bodies were studied by scanning electron microscope (SEM, XL30, Philips Co). The specimens for SEM were polished to a 1 μm surface finish using diamond spray, and thereafter thermally etched for 15 min at 1400 °C in Ar–12%H_2 atmosphere. X-ray diffraction was carried out in the range of $15 < 2\theta < 80$ using Philips X-pert model with Cu K_α radiation. The density of the sintered material was determined by the Archimedean method using distilled water.

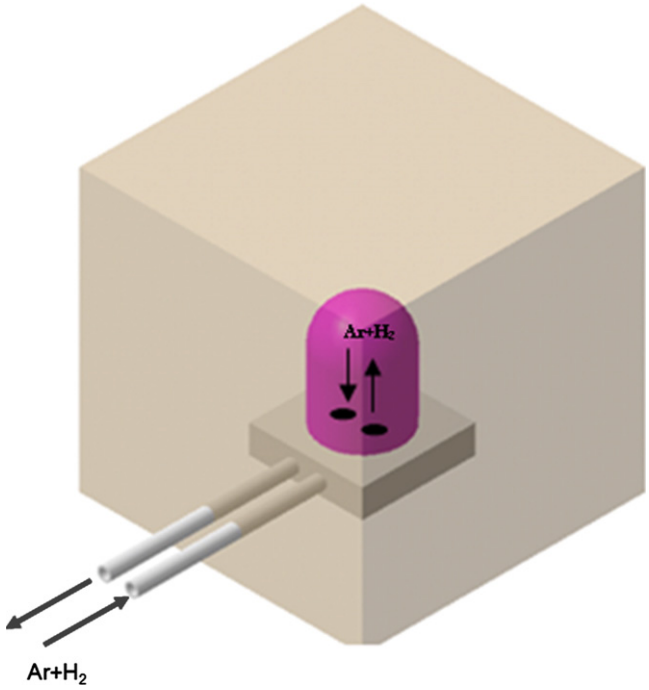

Fig. 1. Schematic of the reaction system.

The strength was determined by three-point bending. The sintered bars (2.5 mm by 5 mm by 25 mm) were polished to 1 μm. The flexural strength was conducted in air at room temperature (Instron Universal Testing Machine-1196) with a crosshead speed of 1 mm/min. At least seven specimens were tested for each series of composition. The hardness was measured by Vickers indentation (Hv) on polished surfaces with an indentation load of 5 kg and loading time 15 s.

3. Results and discussion

The X-ray diffraction patterns of the gel heat treated at temperature range of 1250–1600 °C for 2 h is illustrated in Fig. 3. As is shown, mullite and corundum peaks can be detected at 1250 °C and the intensity of these phases increases up to 1450 °C. Increasing the temperature up to 1600 °C, resultes in disappearance of the peaks related to mullite and appearance of SiC peaks. The more probable reactions of the xerogel during the heat treatment are:

$$SiO_2(s) + 3Al_2O_3(s) = 3Al_2O_3 \cdot 2SiO_2(s) \quad (1)$$

$$Al_2O_3 \cdot 2SiO_2(s) + 6C(s) = 3Al_2O_3(s) + 2SiC + 4CO \quad (2)$$

The thermodynamic analysis of the reactions (1) and (2) is performed according to Gibbs–Helmholts equation: $\Delta G = \Delta H - T\Delta S$. Pressure value of gas phases are took 0.1 MPa for the simplification of calculation. The relationship between the change of Gibbs-free energy and temperature is shown in Fig. 4. It can be seen that ΔG for reaction (1) keeps negative at the temperatures higher than

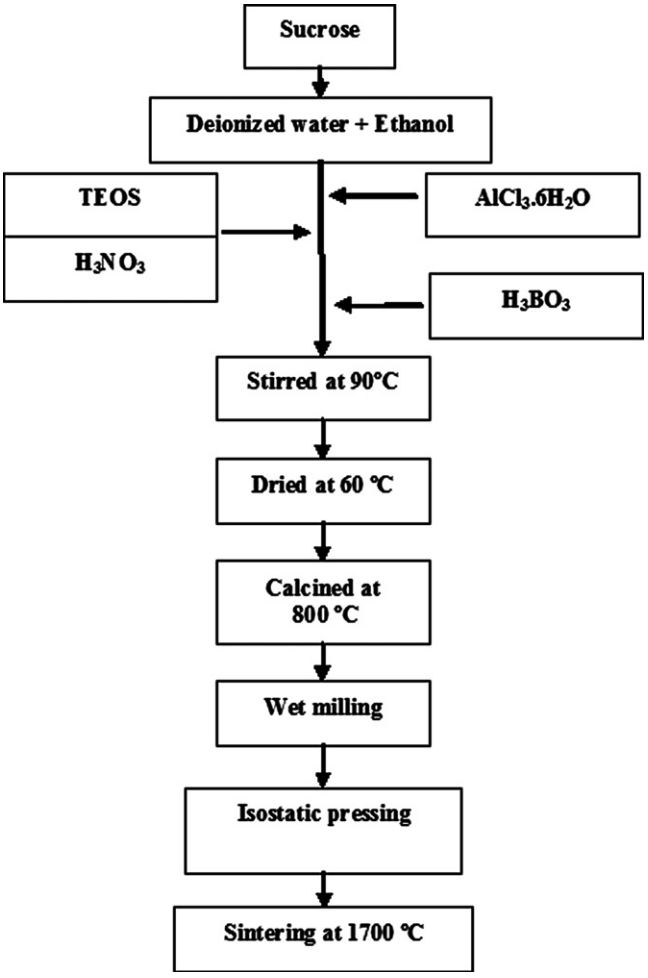

Fig. 2. The flow chart of the processing of Al_2O_3–SiC nanocomposite.

Table 1
Composition of sintered specimens.

Specimen		B_2O_3 (wt%)	Alumina (vol%)	SiC (vol%)
SB0	S5B0	0	95	5
	S10B0	0	90	10
SB1	S5B1	1	95	5
	S10B1	1	90	10
SB3	S5B3	3	95	5
	S10B3	3	90	10

700 °C. So, mullite can be formed at any temperature higher than 700 °C. For reaction (2), ΔG decreases with increasing temperature and turns negative when temperature rises to 1560 °C. Accordingly, SiC can be synthesized through mullite and carbon reaction above 1560 °C. This is in agreement with the peaks indicated in the XRD patterns at 1600 °C.

Upon heating, H_3BO_3 decomposes to B_2O_3 which is thoroughly miscible in SiO_2. It can be seen from the phase diagram of Al_2O_3–B_2O_3–SiO_2 that mullite and liquid phase

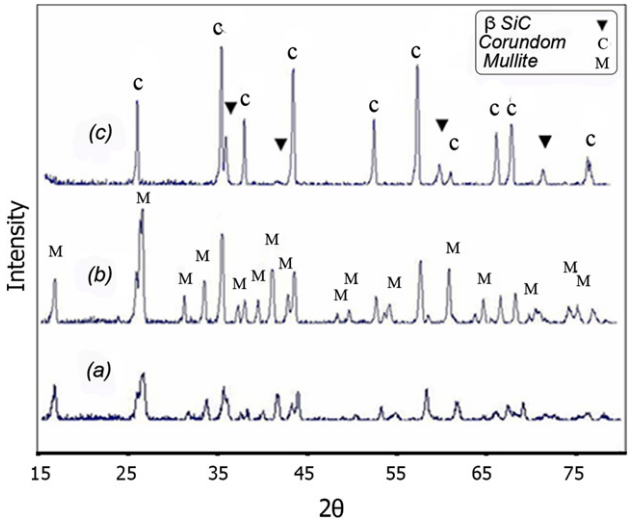

Fig. 3. XRD pattern of dried gel, heat treated at (a) 1250 °C, (b) 1400 °C, (c) 1600 °C for 2.5 h.

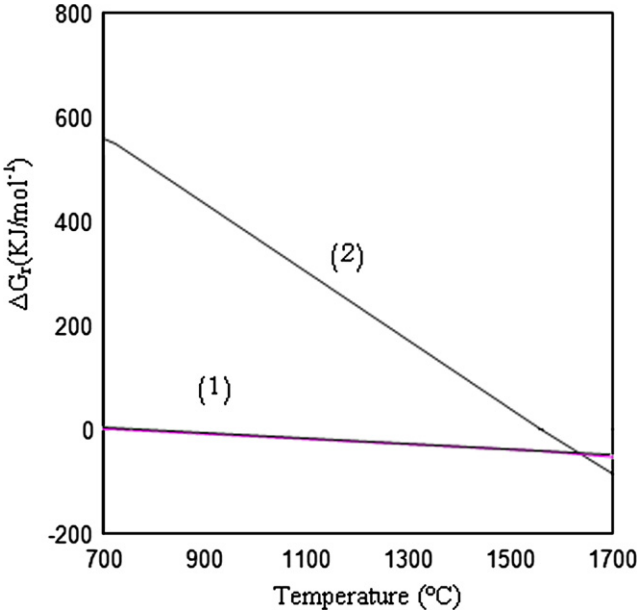

Fig. 4. ΔG_r for possible reactions at different tempetatures.

exist at the temperatures lower than 1700 °C in a wide range of compositions (Fig. 5(a)). In the isothermal section at 1600 °C (Fig. 5(b)), it is evident that the presence of B_2O_3 results in the formation of the liquid phase on the mullite surface. Fig. 6 shows the SEM micrograph of the S5B3 specimen heat treated at temperature range of 1400–1700 °C. The needle like mullite crystals can be identified at 1400 °C, and the mullite and alumina phases surrounded by the liquid phase can be seen at 1500 °C. Raising the temperature up to 1600 °C results in the appearance of SiC nanoparticles. The liquid phase, which is formed during sintering, can wet the solid phases, and the pores in the compact can be largely surrounded by the liquid. In the initial stage of sintering, the liquid fills the pores, breaks up particle contacts and removes inter-particle friction [28].

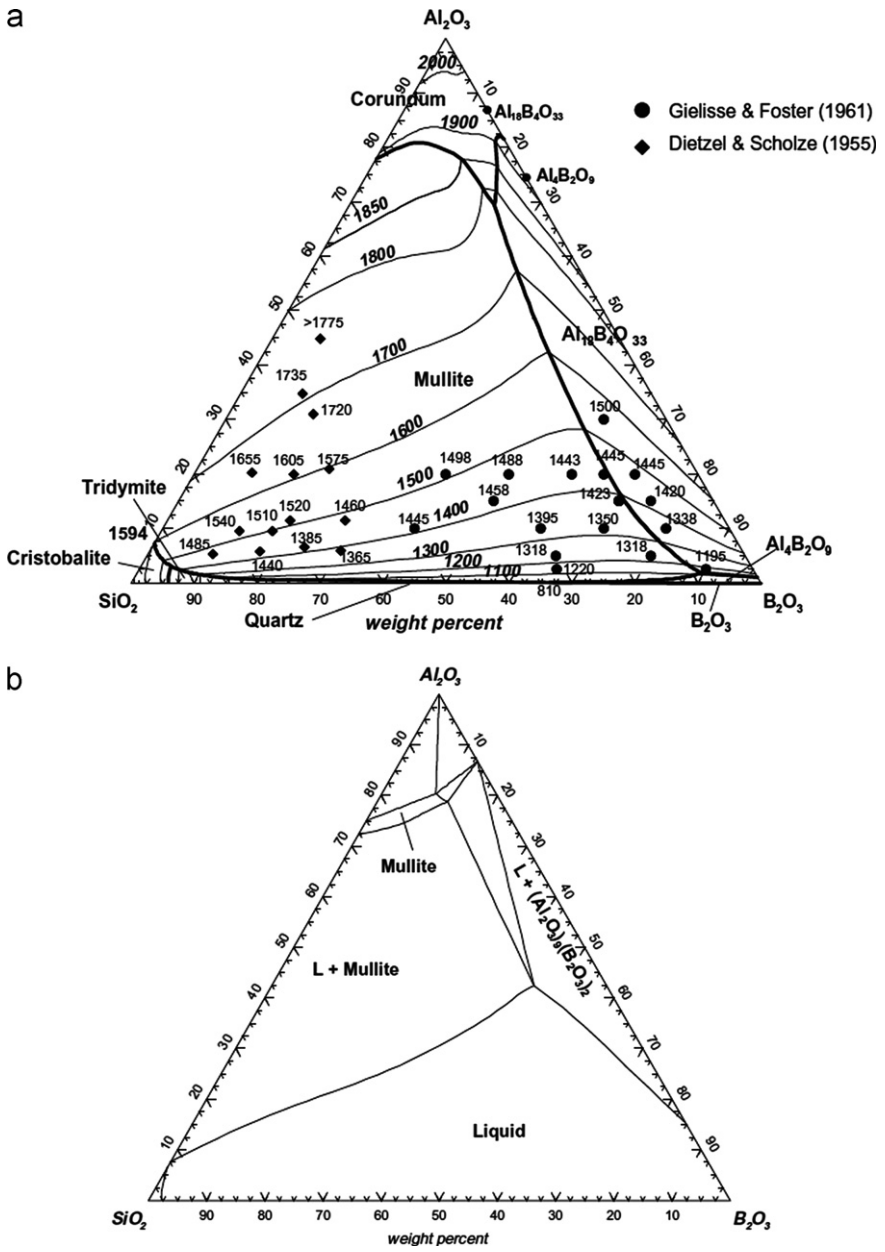

Fig. 5. (a) Phase diagram of the Al_2O_3–B_2O_3–SiO_2 system, (b) isothermal section of the Al_2O_3–B_2O_3–SiO_2 system at 1600 °C [28].

Accordingly, the liquid which surrounds the needle-like mullite phase can promote the solution of mullite and precipitation of SiC nanoparticles in the intermediate stage of sintering. This liquid phase make the diffusion process more active, and allow more frequent and efficient contacts between mullite and carbon. So, it may enhance the reactions of SiC formation [25,26] and improve the densification process as a result.

Fig. 7 shows the effect of B_2O_3 addition on the densification of the specimens sintered at 1700 °C. The two composite materials containing 5 vol% SiC doped with B_2O_3 reach 98.7% (3 wt% B_2O_3) and 96.8% (1 wt% B_2O_3), while the undoped one reaches only 96% of full density. The effect of B_2O_3 addition is less pronounced in Al_2O_3–10 vol% SiC. The undoped composite only reaches 91%, and the two composites doped with 1 wt% and 3 wt% B_2O_3 reach 91.3 and 92.1% of full density, respectively. It seams that when the volume fraction of SiC increases to 10%, the amount of the liquid phase formed with the addition of 1 and 3 wt% B_2O_3 is not sufficient to enhance the material transport processes. It can also be observed from the figure that the relative density of the specimens decreases by increasing the SiC volume fraction. It is well established that the presence of SiC particles will inhibit the densification and grain growth of Al_2O_3 because SiC particles are immobile and do not react with Al_2O_3 during the sintering temperature, so they made the movement of the grain boundaries difficult. Moreover, the reactions of SiC formation and phase transformation of alumina, takes place during sintering

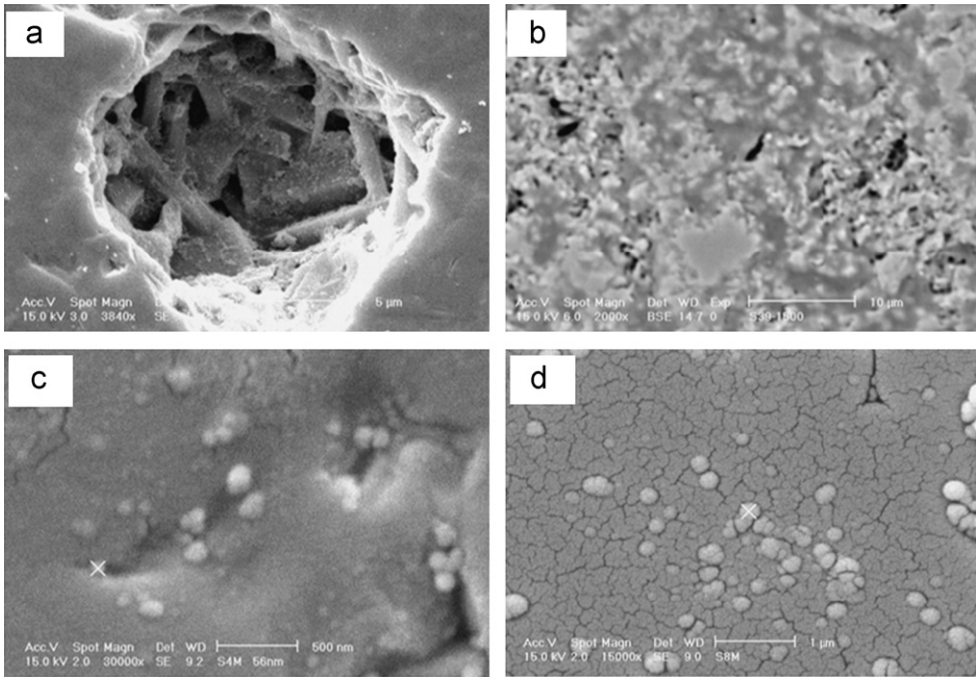

Fig. 6. SEM micrograph of the S5B3 specimen heat treated at (a) 1400 °C, (b) 1500 °C, (c) 1600 °C, (d) 1700 °C for 2.5 h.

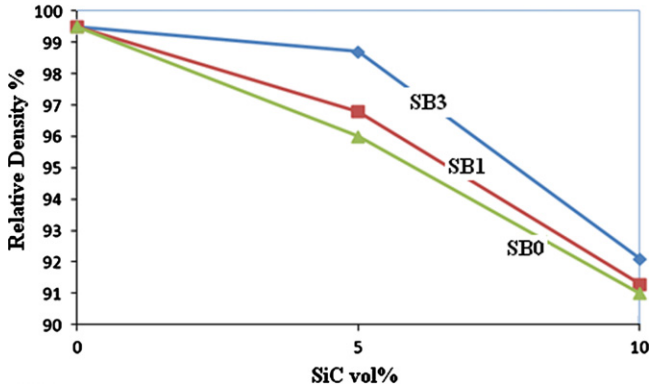

Fig. 7. Relative density of SB0, SB1 and SB3 samples sintered at 1700 °C for 2.5 h.

process. Presence of other phases could postpone the formation of αAl_2O_3 [29] and as a consequence may delay the densification process. When diffusion process becomes active enough for densification, the phase transformation and reactions of SiC formation are already energetically possible and favored [30]. So discernable densification takes place after phase transformation and the sintering temperature had to be raised by increasing the volume fraction of SiC.

Backscattered SEM micrograph of S5B3 specimen sintered at 1700 °C is illustrated in Fig. 8. As can be seen, the liquid phase exists in the grain boundaries, and some of the larger SiC particles can be identified in the microstructure. These nanoparticles are well dispersed in the microstructure, and the agglomerated and large particles located in the grain boundaries.

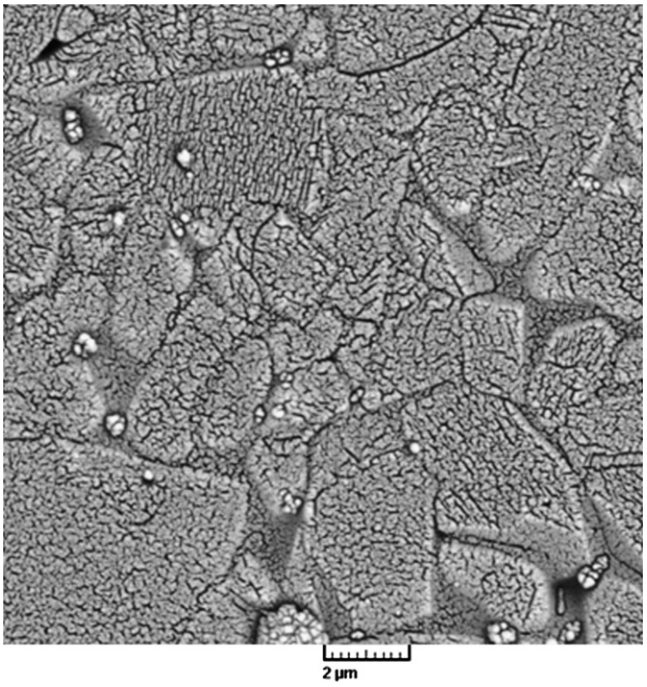

Fig.8. Backscattered SEM micrograph of S5B3 specimen sintered at 1700 °C for 2.5 h.

SEM micrographs of the composites sintered at 1700 °C and etched at 1400 °C are illustrated in Fig. 9. As can be seen, increasing the SiC content results in decreasing the grain size of alumina in the microstructure of the SB0 samples, while this effect is less pronounced in SB1 and SB3 specimens. In solid-state sintering, the grain growth can be effectively inhibited by introducing particles of a

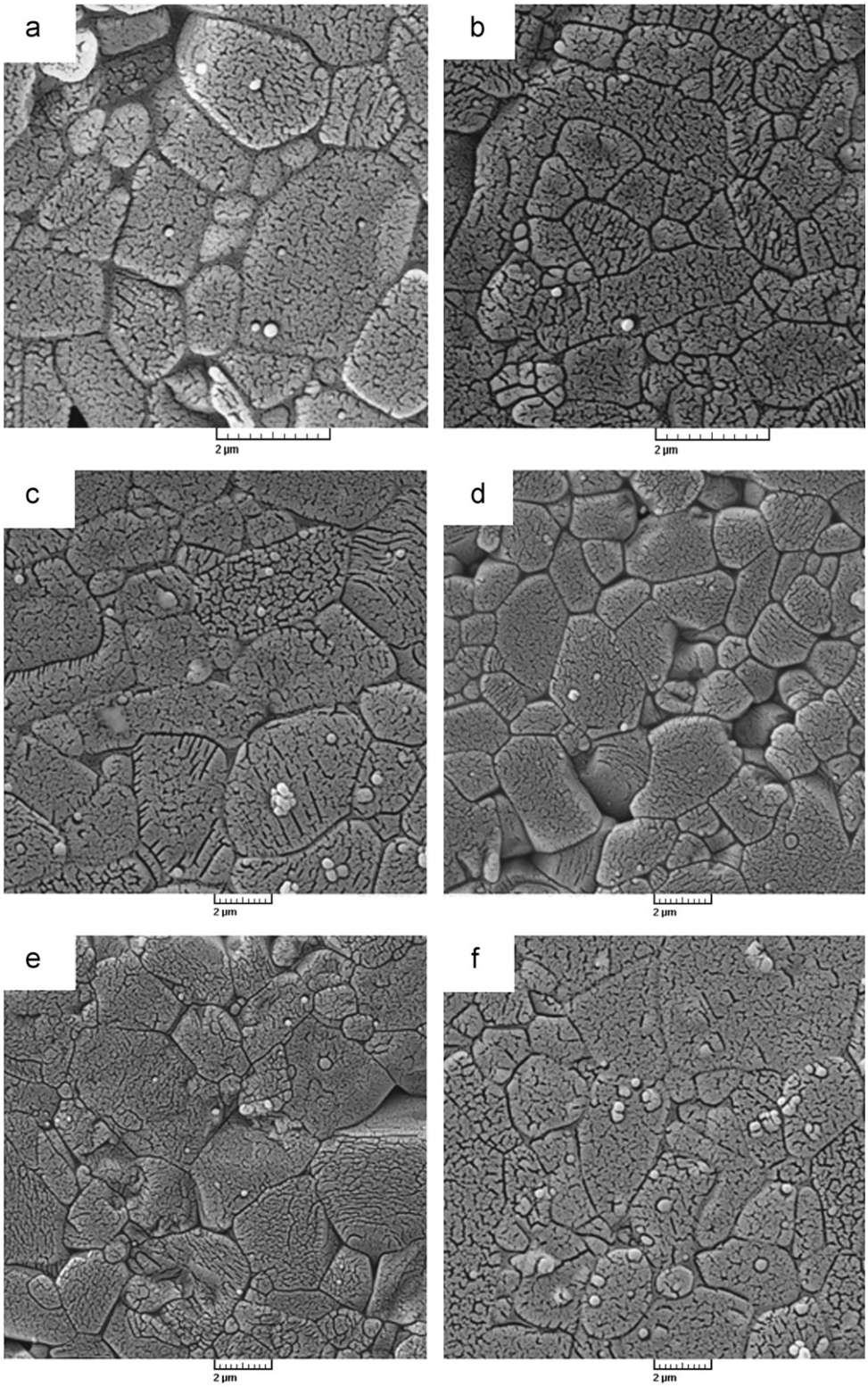

Fig. 9. SEM micrograph of (a) S5B0, (b) S10B0, (c) S5B1, (d) S10B1, (e) S5B3, (f) S10B3 specimens sintered at 1700 °C for 2.5 h.

second solid phase [17] which does not normally have a significant effect on the liquid phase densification mechanism. In-situ synthesized SiC nanoparticles are identified in all samples. These particles are spherical in shape and located predominantly to the interior of matrix grains.

Fig. 10 shows the effect of B_2O_3 addition on the flexural strength of the Al_2O_3–5 vol% SiC specimens sintered at 1700 °C. The flexural strength was observed to increase, with increase in B_2O_3 content. As is known the mechanical properties of ceramic materials depends on the density of

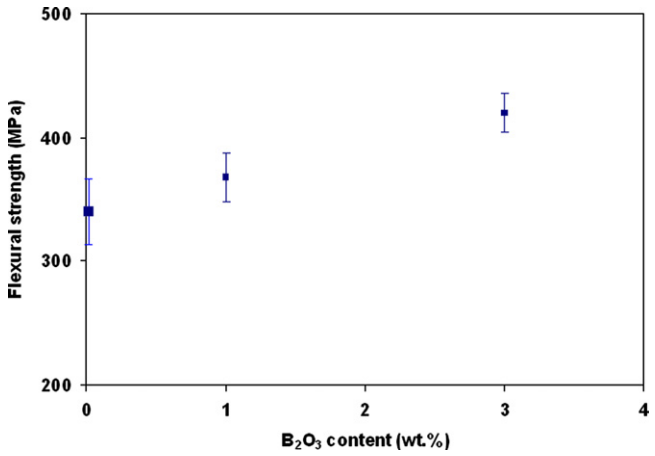

Fig. 10. The effect of B_2O_3 addition on the flexural strength of the Al_2O_3–5 vol% SiC specimens sintered at 1700 °C for 2.5 h.

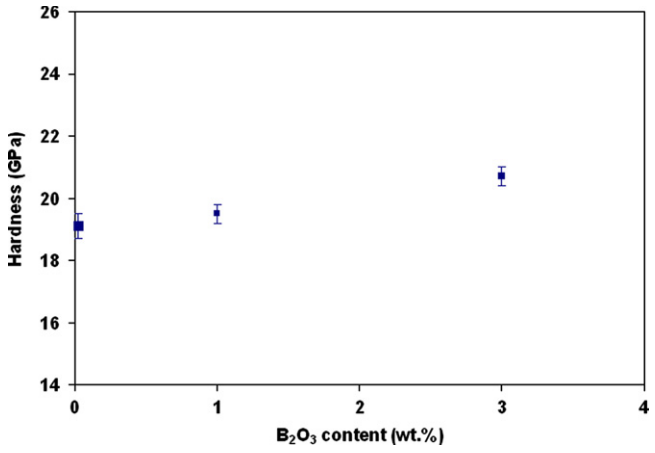

Fig. 11. The hardness of the Al_2O_3–5 vol% SiC samples sintered at 1700 °C for 2.5 h as a function of B_2O_3 contents.

the samples and microstructural characteristics [31]. In this work the improvement in flexural strength is due to the effect of B_2O_3 on increase of relative density (Fig. 7.). It implies that, the strength in Al_2O_3–5 vol% SiC specimen is limited by factors such as the presence of porosities and flaws which limit the strength improvement with mixed powder routes.

Fig. 11 presents the hardness of the Al_2O_3–5 vol% SiC samples as a function of B_2O_3 contents. A trend similar to the flexural strength was observed for the hardness. The higher hardness of the composite with 3 wt% B_2O_3 may be due to the higher density of the sample.

4. Conclusions

The results highlight the potential of fabricating a dense Al_2O_3–SiC nanocomposite with a homogenous distribution of SiC nanoparticles formed in-situ during pressureless sintering of alumina-silica gel-derived powders. Addition of B_2O_3 (1 or 3 wt%) is an effective densification aid in the Al_2O_3–5 vol% SiC composites while the densities of doped and undoped Al_2O_3–10 vol% SiC are almost the same. The composite material containing 5 vol% SiC doped with 3 wt% B_2O_3 reaches 98.7% of full density. Nanosized β-SiC can be formed by means of a reaction between mullite and carbon at 1600 °C. Addition of B_2O_3 leads to formation of the liquid phase that surrounds the needle-like mullite phase. This liquid phase can promote the solution of mullite and precipitation of SiC nanoparticles. The mechanical properties of the composites were improved by adding B_2O_3.

References

[1] K. Niihara, New design concept of structural ceramics–ceramic nanocomposites, Journal of the Ceramic Society of Japan 99 (10) (1991) 974–982.
[2] J. Homeny, W.L. Vaughn, Silicon carbide whisker–alumina composites; effect of whiskers surface treatment on fracture toughness, Journal of the American Ceramic Society 73 (2) (1990) 394–402.
[3] R. Bermejo, A.J. Sánchez-Herencia, L. Llanes, C. Baudín, High-temperature mechanical behavior of flaw tolerant alumina–zirconia multilayered ceramics, Acta Materialia 55 (14) (2007) 4891–4901.
[4] J.F. Bartolomé, C.F. Gutiérrez-González, R. Torrecillas, Mechanical properties of alumina–zirconia–Nb micro–nano-hybrid composites, Composites Science and Technology 68 (6) (2008) 1392–1398.
[5] L.P. Ferroni, G. Pezzotti, Evidence for bulk residual stress strengthening in Al_2O_3/SiC nanocomposites, Journal of the American Ceramic Society 85 (8) (2002) 2033–2038.
[6] H. Reveron, O. Zaafrani, G. Fantozzi, Microstructure development, hardness, toughness and creep behaviour of pressureless sintered alumina/SiC micro–nanocomposites obtained by slip-casting, Journal of the European Ceramic Society 30 (6) (2010) 1351–1357.
[7] H. Awaji, S.M. Choi, E. Yagi, Mechanisms of toughening and strengthening in ceramic-based nanocomposites, Mechanics of Materials 34 (7) (2002) 411–422.
[8] B. Li, J. Deng, Addition of Zr–O–B compounds to improve the performances of alumina matrix ceramic materials, Journal of Alloys and Compounds 473 (1-2) (2009) 190–194.
[9] Y.J. Lin, C.P. Tsang, The effects of starting precursors on the carbothermal synthesis of SiC powders, Ceramics International 29 (1) (2003) 69–75.
[10] S.A. Hassanzadeh-Tabrizi, E. Taheri-Nassaj, Synthesis of an alumina–YAG nanopowder via sol-gel method, Journal of Alloys and Compounds 456 (1-2) (2008) 282–285.
[11] S.A. Hassanzadeh-Tabrizi, E. Taheri-Nassaj, Sol-gel synthesis and characterization of Al_2O_3–CeO_2 composite nanopowder, Journal of Alloys and Compounds 494 (1-2) (2010) 289–294.
[12] A. Taavoni-Gilan, E. Taheri-Nassaj, H. Akhondi, The effect of zirconia content on properties of Al_2O_3–ZrO_2 (Y_2O_3) composite nanopowders synthesized by aqueous sol-gel method, Journal of Non-Crystalline Solids 355 (4–5) (2009) 311–316.
[13] S. Rasouli, E. Taheri-nassaj, In-situ preparation of Al_2O_3–SiC nanocomposites via sol-gel method followed by pressureless sintering, Journal of Alloys and Compounds 496 (1-2) (2010) 678–682.
[14] S. Gustafsson, L.K.L. Falk, E. Lide, E. Carlstro, Pressureless sintered Al_2O_3–SiC nanocomposites, Ceram. Int. 34 (7) (2008) 1609–1615.
[15] J.H. Chae, K.H. Kim, Y.H. Choa, J. Matsushita, J.W. Yoon, K.B. Shim, Microstructural evolution of Al_2O_3–SiC nanocomposites during spark plasma sintering, Journal of Alloys and Compounds 413 (1-2) (2006) 259–264.
[16] Y.L. Dong, F.M. Xu, X.L. Shi, C. Zhang, Z.J. Zhang, J.M. Yang, Y. Tan, Fabrication and mechanical properties of nano-/micro-sized Al_2O_3/SiC composites, Materials Science and Engineering: A 504 (1-2) (2009) 49–54.

[17] S. Gustafsson, L.K.L. Falk, E. Lidén, E. Carlstro, Alumina/silicon carbide composites fabricated via in-situ synthesis of nano-sized SiC particles, Ceramics International 35 (3) (2009) 1293–1296.
[18] D. Galusek, J. Sedlacek, R. Riedel, Al_2O_3–SiC composites prepared by warm pressing and sintering of an organosilicon polymer-coated alumina powder, Journal of the European Ceramic Society 27 (6) (2007) 2385–2392.
[19] H.S. Kim, M.K. Kim, S.B. Kang, S.H. Ahn, K.W. Nam, Bending strength and crack-healing behavior of Al_2O_3/SiC composites ceramics, Materials Science and Engineering: A 483-484 (2008) 672–675.
[20] A. Limpichaipanit, R. Todd, The relationship between microstructure, fracture and abrasive wear in Al_2O_3/SiC nanocomposites and microcomposites containing 5 and 10% SiC, Journal of the European Ceramic Society 29 (13) (2009) 2841–2848.
[21] Perez-Rigueiro, J.Y. Pastor, J. Liorca, M. Elices, P. Miranzo, J.S. Moya, Revisiting the mechanical behavior of alumina-silicon carbide nanocomposites, Acta Materialia 46 (15) (1998) 5399–5411.
[22] J. Wang, S.Y. Lim, S.C. Chew, L.M. Gan, Dramatic effect of a small amount of MgO addition on the sintering of Al_2O_3–5 vol% SiC nanocomposite, Materials Letters 33 (5-6) (1998) 273–277.
[23] S.K.C. Pillai1, B. Baron, M.J. Pomeroy, S. Hampshire, Effect of oxide dopants on densification, microstructure and mechanical properties of alumina-silicon carbide nanocomposite ceramics prepared by pressureless sintering, Journal of the European Ceramic Society 24 (12) (2004) 3317–3326.
[24] I.P. Shapiro, R.I. Todd, J.M. Titchmarsh, S.G. Roberts, Effects of Y2O3 additives and powder purity on the densification and grain boundary composition of Al_2O_3/SiC nanocomposites, Journal of the European Ceramic Society 29 (9) (2009) 1613–1624.
[25] A. Julbe, A. Larbot, C. Guizard, L. Cot, Effect of boric acid addition in colloidal sol-gel derived SiC precursors,J. Charpin, P. Bergez, Materials Research Bulletin 25 (5) (1990) 601–609.
[26] L. Cerovic, S.K. Milonjic, S.P. Zec, A comparison of sol-gel derived silicon carbide powders from saccharose and activated carbon, Ceramics International 21 (4) (1995) 271–276.
[27] Varghese Swamy, In-Ho Jung, Sergei A. Decterov, Thermodynamic modeling of the Al_2O_3–B_2O_3–SiO_2 system, Journal of Non-Crystalline Solids 355 (34-36) (2009) 1679–1686.
[28] R. Warren, R. Lundberg, Principles of preparation of ceramic matrix composites, in: R. Warren (Ed.), Ceramic Matrix Composites, Chapman and Hall, New York, 1992, pp. 35–59.
[29] S. Jiansirisomboon, K.J.D. MacKenzie, Sol-gel processing and phase characterization of Al_2O_3 and Al_2O_3/SiC nanocomposite powders, Materials Research Bulletin 41 (2006) 791–803.
[30] C.Carry Bowen, From powders to sintered pieces: forming, transformations and sintering of nanostructured ceramic oxides, Powder Technology 128 (2-3) (2002) 248–255.
[31] S.A. Hassanzadeh-Tabrizi, E. Taheri-Nassaj, The compaction, sintering, and mechanical properties of Al_2O_3–CeO_2 composite nanopowders, Journal of the American Ceramic Society 94 (10) (2011) 3488–3493.